



# Computational Approaches for Identification of Potential Inhibitors against Rheumatoid Arthritis Causing Gene Janus Kinase2

**Anbuselvam Mohan<sup>1\*</sup>; Wilson Jerica<sup>2#</sup>; Anbuselvam Jeeva<sup>3</sup>; Hai-Feng Ji<sup>2</sup>**

<sup>1</sup>Department of Biotechnology, Selvamm Arts and Science College (Autonomous), Namakkal-637 003, Tamil Nadu, India.

<sup>2</sup>Department of Chemistry, Drexel University, Philadelphia, PA 19104, USA.

<sup>3</sup>Department of Biotechnology, Sengundhar Arts and Science College, Tiruchengode-637205, Tamil Nadu, India.

## \*Corresponding Author(s): Anbuselvam Mohan

Assistant Professor, Department of Biotechnology,  
Selvamm Arts and Science College (Autonomous),  
Tamil Nadu, India.

Email: mohanbio33@gmail.com

# Equal to First Author

Received: Jan 10, 2022

Accepted: Feb 21, 2022

Published Online: Feb 25, 2022

Journal: Journal of Nanomedicine

Publisher: MedDocs Publishers LLC

Online edition: <http://meddocsonline.org/>

Copyright: © Mohan A (2022). This Article is distributed  
under the terms of Creative

Commons Attribution 4.0 International License

**Keywords:** Rheumatoid arthritis; JAK2; Database screening;  
ADME; Molecular dynamics.

## Abstract

Rheumatoid arthritis is a chronic autoimmune illness, predominantly affecting elder women over men. Janus Kinase 2 (JAK2) is a non-receptor tyrosine kinase, belonging to the Janus kinase (JAK) family involved in the activation of the JAK/STAT signaling pathway and it plays an important role in several biological processes, such as cell proliferation, differentiation, apoptosis, and physiological and pathological activity. Point mutation occurring in the JAK2 kinase domain derails the normal kinase activity and leads to the progression of rheumatoid arthritis. JAK2 is recognized as a well-validated therapeutic target for the treatment of rheumatoid arthritis. In this study, we applied dynamic computational approaches to identify a new structural scaffold of potential inhibitors for JAK2. We executed structure-based virtual screening and identified four hit compounds from the NCI database screened against JAK2. The top hit compounds were subsequently subjected to ADME prediction studies as part of an evaluation of the druggability; all four hit compounds were found to fall within satisfactory range with predicted pharmacokinetic properties. Eventually, we examined the dynamic behavior of the protein-ligand complexes at different time scales by using the Schrödinger Desmond molecular dynamics package. A molecular dynamics simulation run for 100ns was carried out and results were analyzed using Root Mean Square Deviation (RMSD) and Root Mean Square Fluctuation (RMSF), to signify the stability of the protein-ligand complex. The stability of the protein-ligand complex was higher throughout the entire simulation and the key residues, GLU 930, TYR 931 and LEU 932, play a significant role in the stabilization enhancement of the protein-ligand complex during the course of the simulation. From the outcomes of the computational analyses, we propose the identified inhibitors are extremely suitable for further preclinical and clinical analysis.



**Cite this article:** Mohan A, Jerica W, Jeeva A, Ji HF. Computational Approaches for Identification of Potential Inhibitors against Rheumatoid Arthritis Causing Gene Janus Kinase2. J Nanomed. 2022; 5(1): 1054.

## Introduction

Worldwide, Rheumatoid Arthritis (RA) is a common chronic, symmetrical, inflammatory autoimmune joint disease that predominantly assails elder women versus men. It initially assaults the small joints, connective tissue, muscles, fibrous tissue and tendons; further, it destroys the bones and cartilage of joints and leads to drastically affect large joints. The disease will eventually affect major organs including the skin, kidneys, heart and lungs, and ultimately lead to disability [1,2]. The most common signs of RA are prolonged morning stiffness, fatigue, fever, weight loss, and swollen and/or warm joints. Rheumatoid arthritis affects 1.3 million people in the US. The inflicted rate of RA in women is three times higher than in men [3]. Janus Kinase (JAK) is a non-receptor tyrosine kinase family that is further assorted into four clusters: JAK1, JAK2, JAK3 and TYK2. Among the JAK family, JAK1 and JAK2 widely exist in cells and tissue, while the expression of JAK3 is mainly in myeloid and lymphoid cells [4]. JAK2 is a cytosolic protein located at chromosome 9, with a mass of 130 kDa it comprises of 1,132 amino acids. There are four distinct regions observed in the JAK2 receptor [5]. The first is the highly conserved kinase domain, JH1 (JAK homology1), at the C-terminal region which consists of the activation loop, primary phosphorylation sites, and the ATP binding site. The second is JH2 (JAK homology 2), the pseudo kinase domain, which also has similar structural properties to the kinase domain but lacks catalytic activity. The pseudokinase domain has a structural feature unique to the JAK family. Adjacent to the JH2 domain is the SH2 (Src Homology 2)-like domain, whose function is not yet fully investigated. The final region is the FERM domain located at the N-terminus, which is mainly responsible for interactions between JAK2 and a number of cell surface receptors. JAK2 could not trigger the biological activity unless signaling molecules bind with JAK2. JAK2 possesses a ligand-dependent mechanism and is mainly activated by several crucial signaling molecules such as erythropoietin, thrombopoietin, growth hormone, interferon  $\gamma$ , interleukin-3 and leptin. The signaling molecules bind with the receptor site of the cell and trigger the activation of the receptor dimerization and phosphorylation of JAK2, generating the binding site for STAT (Signal Transducer and Activator of Transcription), STAT is phosphorylated and homo/hetero/multi dimerization after that STAT penetrates the nuclear membrane in the form of homo-hetero dimerization then bind with DNA and involved in the gene transcription and protein synthesis process and produce their specific cytokine signaling activity. The activated JAK-STAT pathway is involved in a variety of normal pathophysiological activities such as hematopoiesis, and cellular metabolism, growth, and proliferation [6]. Any chromosomal aberration occurring in the kinase domain can lead to the dysregulation of JAK2. The abnormal activity of JAK2-STATs signaling pathways leads to the development of various diseases. In particular, point mutation occurring in the position of V617F located at the kinase domain of JAK2 have been predominantly implicated in various diseases such as rheumatoid arthritis, psoriasis, and several cancers including breast, prostate, head and neck, myeloid and lymphoid leukemia and Myeloproliferative Neoplasms (MPN) [7]. Our mission is to protect the elderly from the effects of RA. JAK2 is the recognized therapeutic target for rheumatoid arthritis. So far, several JAK2 inhibitors have been developed for rheumatoid arthritis such as ruxolitinib, pacritinib, and AZD1480 but the adverse effects of these drugs, which includes anemia (platelets, red and white blood cells), hypercholesterolemia; increased transglutaminases and creatinine levels, and an increase in common

infections like herpes zoster, herpes simplex, urinary tract infections, and gastroenteritis, demonstrates the immense need for effective inhibitors for RA and novel approaches to treatment [8,9]. The discovery of effective drug candidates is a high-risk, expensive, and lengthy process, taking around 14 years with a minimum cost of 800 million US dollars. Currently computer-aided drug design plays a significant role in the discovery of innovative potential drug candidates before ever engaging in wet-lab research. In this work, we applied *in silico* methods including virtual screening, ADME properties filtration and molecular dynamic simulations to identify potential hit molecules from the NCI compound database.

## Materials and methods

### Preparation and grid generation of target protein structure

Preparation of the target protein structure is one of the essential steps before undertaking docking to reduce steric hindrance. The crystal structure of the arthritis causative protein, JAK2, was downloaded from RCSB Protein Data Bank (RCSB PDB, <http://www.rcsb.org/>; PDB ID: 3KRR; co-crystal ligand: NVP-BSK805; Resolution: 1.80Å; R-Value free: 0.206 and R-Value: 0.167) [10]. The downloaded JAK2 crystal structure was imported and prepped using Schrödinger's Maestro protein preparation wizard. In this structural refinement process, the integrity of the target protein structure was checked and adjusted, hydrogen atoms were added, bond order was adjusted, and the co-crystallized water molecules and ligand were removed from the target structure of JAK2. Finally, the protein structure energy was minimized using the OPLS3 force field until the RMSD cut-off was touched at 0.30Å [11]. The prepared protein structure was taken into the receptor grid generation panel for grid generation. The binding site concave region possess some ideal chemical features which is responsible for interaction of ligands and explore desired biological activity it may be activation of the suppressed target protein, modulation their activity otherwise inhibits the over expression of particular therapeutic target. Due to this reason, the active site information is crucial for docking [12]. Gathering the binding pocket residues from research articles we determined the following residues: LEU 855, GLY 856, LYS 857, GLY 858, GLY 861, ALA 880, MET 929, GLU 930, TYR 931, LEU 932, PRO 933, TYR 934, GLY 935, SER 936, ARG 980, ASN 981, LEU 983, GLY 993 and ASP 994 were mainly associated with any interactions with bound ligands and were considered for grid generation [13-16]. The information enabled the "Receptor Grid Generation" using the panel of Glide. Further, the grid box was constructed to cover the docking sites of the target protein with a set grid box size of 20Å×20Å×20Å with OPLS 3 force field. The van der Waals scaling factor was set to 1.0 and the partial charge cutoff to 0.25. The constructed grid file was then inputted for the molecular docking studies.

### Preparation of the database ligands

250,000 molecules were downloaded from the NCI database of human cellular signaling pathways in SDF format and imported into Schrödinger's LigPrep for ligand preparation [17]. During this process, the ligands' 2D chemical structures are converted into 3D structures and Ionizer is used to generate possible ionization and protonation states for each ligand at pH7.0  $\pm$ 2.0. Stereoisomers were generated for all ligands with unassigned stereogenic centers, with a limit of 32 stereoisomers considered per ligand, tautomeric states were generated for all conformers with possible prototropic tautomerism [18]. We retained only the lowest energy conformer for each ligand,

this refined group of ligands was channeled into the structure-based virtual screening process for effective hit identification using Schrödinger Glide.

### Virtual screening

Virtual screening is one of the most promising computational methods and is chiefly employed for filtering potential pharmacological hit compounds and eliminating compounds with disagreeable qualities from the large chemical database. Within both academia and industry it is agreed that structure-based virtual screening is an immense, successful, well-validated, and highly attractive strategy applied in the early stages of the drug discovery process for identification of potential hit compounds with the anticipation these pharmacologically efficient hits will generate highly qualified leads from vast chemical libraries against therapeutic targets. Here, we employed Schrödinger Glide for database screening. The ligands are docked and filtered through a series of different precision levels beginning with High Throughput Virtual Screening (HTVS), which is employed for rapid screening. The top hits from HTVS are then isolated and docked using Standard Precision (SP). Then, the top-scoring compounds from SP are docked employing Extra Precision (XP) modes to eliminate any false positives and narrow the selection to the most efficient hits. Glide XP visualizer was used to analyze various protein-ligand interactions such as hydrogen bond interaction, hydrophobic interaction, salt bridge, pi-cation, and pi-pi stacking interactions [19-21]. Finally, the scrutinized the hit compounds were further taken into ADME properties analysis.

### ADME profile assessment

Drug discovery and development is an expensive and high-risk undertaking. Delivering a new drug to market averages 12 years and 800 million US dollars. Typically, 1 in 30 validated lead compounds pass phase I clinical trials, and only 1 in 6 leads become marketable drugs after phase I trials. Overall, a lead compound has only a 5% chance to obtain final FDA approval in the US. Late-stage candidate dropout within the drug discovery process is often due to a potential compound's lack of efficacy, adverse effects, excessive toxicity, poor membrane absorption, penetration, or poor clearance. The termination of the project at any stage of the drug discovery process is an exponential cost loss for pharmaceutical companies and individual drug discovery research groups. Pharmaceutical companies lose millions owing to the termination of a drug discovery project. But, the withdraw of a commercially approved drug from the market leads to waste amounting to billions of dollars. Yearly, within the US, there are 2 million hospitalizations, hundred thousand deaths and thousands of malpractice cases due to adverse drug reactions [22,23]. To combat both the late-stage termination of drug discovery projects and the commercial recall due to adverse effects the early evaluation of a hit compound's Absorption, Distribution, Metabolism and Excretion (ADME) properties is paramount. Assessment of ADME properties is one of the most significant steps in the preliminary phase of drug discovery and development to obtain optimal drug-like candidates for further experimental investigation. Experimental evaluation of the ADME properties is not appropriate for millions of compounds, as it would require a vast increase in manpower, animals, equipment, and time [24,25]. QikProp [26], an *in silico* tool for ADME assessment, was utilized to predict the following properties for the hit compounds: partition coefficient (QPlogP octanol/water), Aqueous Solubility (QP log S), Vander Waals surface area of Polar Nitrogen and Oxygen Atoms (PSA), Lipinski's Rule of Five (LROF), gut-blood brain barrier (QPPCaco2), LogIC50 value for

the blockage of K<sup>+</sup> channels (QPlogHERG), percentage of human oral absorption, LogP (water/gas), molecular weight, hydrogen bond donor, and hydrogen bond acceptor.

### Molecular dynamics

We executed Molecular Dynamics (MD) simulations to investigate the binding stability of the protein-ligand complex by employing Schrödinger's MD simulation package Desmond [27]. We obtained the four JAK2 hit compounds from the aforementioned structure-based virtual screening and input the files for molecular dynamics simulation. The protein-ligand complex was solvated with simple point energy with the help of the OPLS3 force field. The orthorhombic water box was used to create a 10 Å buffer regions between the protein atoms and box sides and the systems were neutralized with Na<sup>+</sup> and Cl<sup>-</sup> ions. The OPLS-2005 force field was used for energy calculation. The temperature was maintained constant at 300 K, and a 2.0 fs value was obtained in the integration step. We executed MD simulations for the complex structure of the protein as well as the target with position restraints for 6000 ps to allow the water molecules to remain in the system. Root-Mean-Square Deviation (RMSD), Root-Mean-Square Fluctuation (RMSF), and total energy of the complexes were analyzed by using event-analysis and simulation-interaction diagrams [28,29].

## Results and discussion

### Selection of inhibitors

The current study employs molecular docking tool Glide to execute virtual screening of compounds from NCI database against JAK2, the most validated therapeutic target to combat rheumatoid arthritis. The study involves three significant filtering steps, namely, High Throughput Virtual Screening (HTVS), Standard Precision (SP), Extra Precision (XP), and scores the ligand binding free energy as a Glide Score in choosing the most useful drug candidate. The virtual screening initiated with downloading 250,000 small molecules from the NCI database and docked into active site of the target protein, JAK2 by using HTVS, SP and XP docking routes and the scores obtained with the native ligand, NVP-BSK805 for the respective parameters. Having superimposed the native ligand on redocked complex using Chimera to obtain the filtering parameter scores depicted in Figure 1. Initially, we obtained 50,000 compounds from the HTVS mode based on the reference ligand score -5.25 kcal/mol. The ligand molecules were further filtered by docked with JAK2 active site based on reference ligand SP score -6.24 kcal/mol by using SP docking mode, finally, the 5000 compounds were docked into active site region of target protein JAK2, In this XP mode, 50 compounds had a designated Glide Score better than the reference score, -8.54 kcal/mol of the native ligand. Subsequently, the 50 ligands were subjected to ADME properties analysis. Finally, four compounds were identified with adequate ADME properties. The Glide Score, Glide Energy, interacting residues, and their distance for the four best hit compounds are stated in Table 1 and the hydrogen bond, hydrophobic interactions of the four hit compounds are displayed in Figure 2-5. The 2D structures of the ligands were depicted in Figure 6. These four hit compounds are: 62052 or 2-[1-(Pyridin-3-ylmethylene-hydrazinocarbonyl)-ethylsulfanyl]-propionicacidpyridin-3-ylmethylene-hydrazide, 353906 or 2,3,8,9-tetramethylquinolino[8,7-h]quinoline-1,7-diol, 87845 or 2-oxo-6-phenyl-4-(2-phenyl ethyl)-1,2-dihydropyridine-3-carbonitrile, and 76746 or Urorosein.

**Table 1:** Glide extra-precision (XP) results for the four molecules by use of Schrödinger 10.2.

S. No	Compound ID	Glide Score (kcalmol <sup>-1</sup> )	Glide Energy (kcalmol <sup>-1</sup> )	No. of hydrogen bonds	Interaction residues	Distance (Å)
1	62052	-9.681	-72.835	4	LEU 855	1.96
					SER 936	1.73
					TYR 931	2.07
					LEU 932	1.98
2	353906	-9.495	-46.506	3	LEU 855	1.95
					GLU 930	1.77
					LEU 932	1.93
3	87845	-8.568	-55.075	2	LEU 932 (2)	2.36
						1.96
4	76746	-8.002	-39.24	1	LEU 932	2.02

The IDs are of the NCI database; Glide score (Kcal/mol); Glide energy (Kcal/mol); Number of hydrogen bond interaction; Interacting residues, Distance.

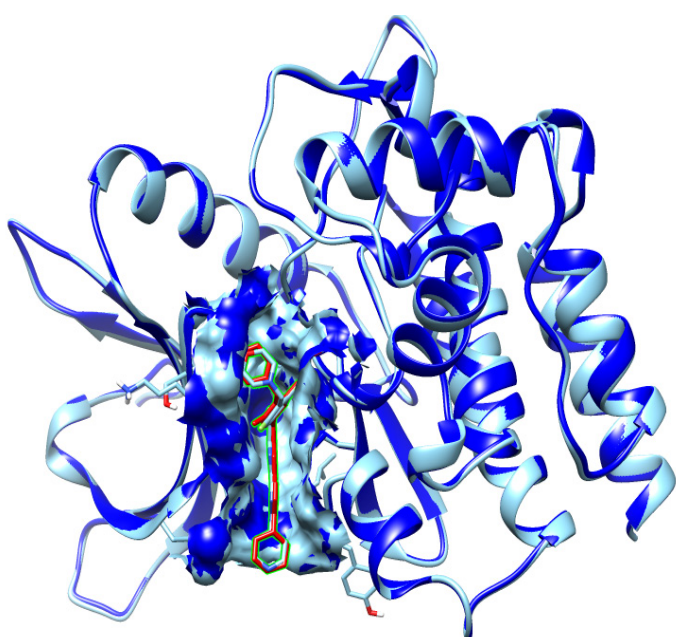


**Figure 1:** The superimposition of re-docked JAK2-NVP-BSK805 (red) onto co-crystallized. Complex (cyan) in the active site using Chimera (RMSD = 0.153Å).

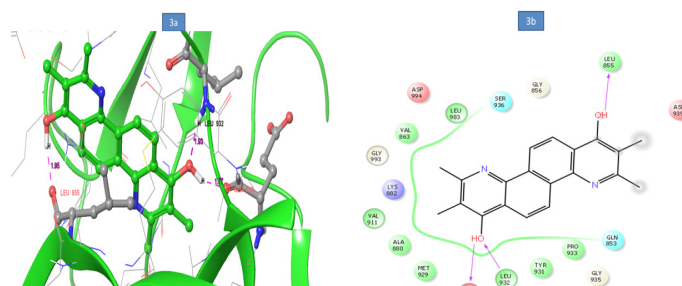


**Figure 3:** (a) 3-D interaction diagram of the Janus kinase2 and 353906, (b) 2-D interaction diagram of the Janus kinase2 and 353906

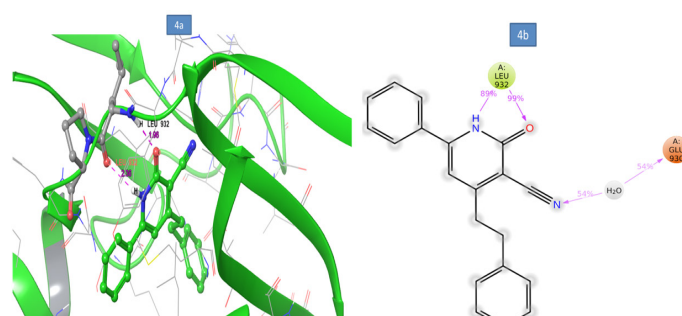


**Figure 4:** (a) 3-D interaction diagram of the Janus kinase2 and 87845, (b) 2-D interaction diagram of the Janus kinase2 and 87845.

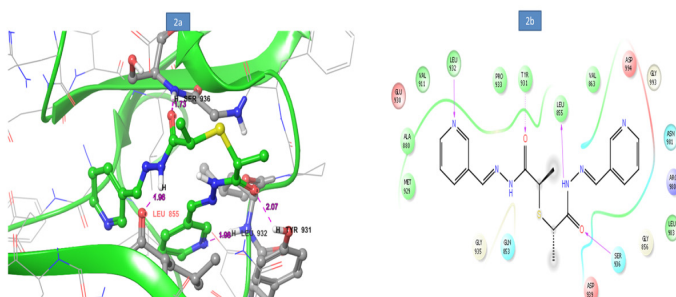


**Figure 2:** (a) 3-D interaction diagram of the Janus kinase2 and 62052, (b) 2-D interaction diagram of the Janus kinase2 and 62052.

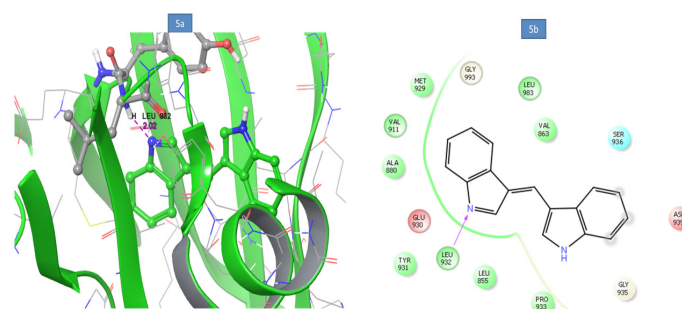


**Figure 5:** (a) 3-D interaction diagram of the Janus kinase2 and 76746, (b) 2-D interaction diagram of the Janus kinase2 and 76746.

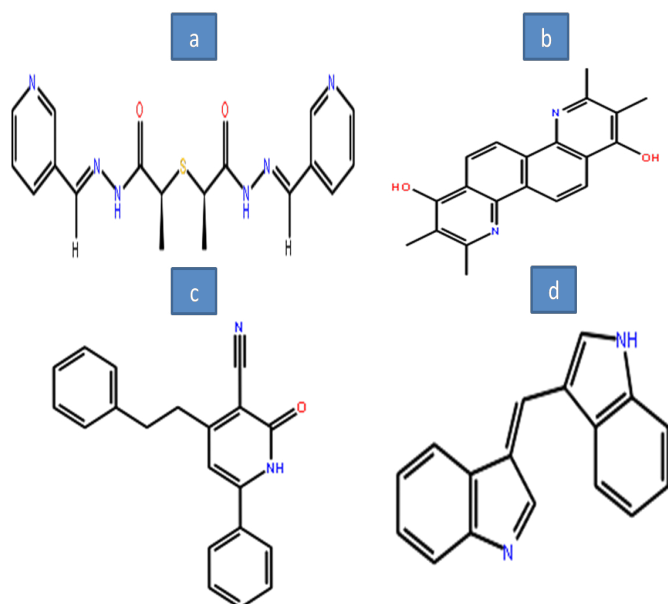


**Figure 6:** 2D diagram of virtual screening hits (a) 62052; (b) 353906; (c) 87845; (d) 76746.

## Docking studies

### Binding mode of ligand 62052

We examined the binding mode of 62052 within the active site of JAK2 and observed four hydrogen bond interactions formed between the hit compound and the protein. The first hydrogen bond interaction is found between the nitrogen of the first pyridine group of hit compound 62052 and the backbone hydrogen atom of LEU932's amino group, with a bond length of 1.98Å. Following the molecule's structure, the second interaction is found between the first of the symmetrical hydrazide oxygen atoms of compound 62052 and the amino acid residue TYR 931's hydroxyl hydrogen, with a bond length of 2.07Å. Continuing, the hydrogen atom of the secondary amine of the second hydrazide interacts with the carbonyl oxygen of residue LUE 855's backbone, with a bond distance of 1.96Å. And lastly the hydrogen atom of the polar residue of SER 936 interacts with the oxygen atom of the second hydrazide of hit 62052 with a bond distance of 1.73Å. Also note that the key residues, TYR 863, TYR 931, VAL 911, MET 929, LEU 983, PRO 933 and ALA 880, participate in hydrophobic contact with the target structure of JAK2. The Glide Score and glide energy were calculated at -9.681kcal/mol and -72.835kcal/mol respectively. **Binding mode features of the ligand 353906**

The binding mode of 353906 with JAK2 produced three hydrogen bonds. The first hydroxy group hydrogen of the hit compound interacts with the backbone oxygen atom of the residue LUE 855 with a bond length of 1.95Å. The hydrogen atom of the second hydroxyl group interacts with the backbone oxygen atom of the negatively charged residue of GLU 930 with a bond distance of 1.77Å while the oxygen atom of the second hydroxyl group of 353906 interacts with the backbone hydrogen atom of the hydrophobic residue of LEU 932 with a bond distance of 1.93Å. Further, the key residues, PRO 933, TYR 931, MET 929, ALA 880, VAL 911, VAL 863, and LEU 983, are involved in the hydrophobic interactions with JAK2. The Glide Score and glide energy obtained as -9.495 kcal/mol and -46.506 kcal/mol respectively.

### Binding mode of the ligand 87845

The docking analysis of hit compound 87845 within the active site of JAK2, illustrates only two hydrogen bond interactions one with the protein residue LEU 932. The oxygen atom of the hydrophobic residue interacted with the hydrogen atom bound to the nitrogen of the pyridinone ring of the hit compound 87845 with a bond length of 2.36 Å. The second hydrogen bond involves the hydrogen atom of LEU 932 and the ketone oxygen atom of the hit compound 87815 with a bond length of 1.96 Å. The following residues, TYR 931, LEU 983, VAL 911, VAL 863, PRO 933, LEU 855, and ALA 880, were involved in hydrophobic contact with the active site of JAK2. The Glide Score and glide energy observed are -8.568 kcal/mol and -55.075 kcal/mol respectively.

### Binding mode of the ligand 76746

We analyzed the docking simulation of hit compound, 76746 within the active site of the JAK2 producing only one hydrogen bond interaction. The hydrogen atom of the residue LEU 932 interacts with the nitrogen atom of the indole of the hit compound 76746 with a bond length of 2.02 Å. The following residues, MET 929, LEU 983, VAL 863, TYR 931, and LEU 855, are involved in the hydrophobic contact with the active site of JAK2. The Glide Score and glide energy observed were -8.002 kcal/mol and -39.240 kcal/mol respectively.

### Assessment of ADME properties

Drug-like properties of the four hit compounds were assessed to ensure the druggability of the compounds drug development process. The ADME properties of the four hit molecules are obtained using Qikprop. All four hit molecules were found to have desirable drug-like properties based on Lipinski's rule of five which suggests a potential drug candidate has a molecular weight under 500 kDa, contains less than 5 H-bond donors, has less than 10 H-bond acceptors, and a predicted logP below 5. Lipophilicity of a compound is a significant physicochemical property that directly influences the absorption, penetration of biological membrane, aqueous solubility, binding of plasma protein, solubility inside the lipid environment, distribution, and pharmacological potency. The four hit compounds were further evaluated for their drug-like behavior through analysis of additional pharmacokinetic parameters required for efficient Absorption, Distribution, Metabolism, Excretion, and Toxicity (ADMET) by using QikProp. For the four hit molecules, cell permeability (QPpCaco2), a key factor governing drug metabolism and its access to biological membranes, ranged from 529 to 2888. The predicted IC50 value for the blockage of hERG K<sup>+</sup> channels is in the acceptable range below -5. The predicted hERG clearly indicates all the molecules have the desired values and will efficiently cross the hERG channel and provide an electric signal to the heart and the compounds eradicate cardiac arrest. The predicted Brain/Blood barriers are under the acceptable range -1.323 to -0.058 and its efficiently indicate all the compounds having sufficient CNS penetration capabilities, the number of rotatable bonds ranges from 2 to 10, the predicted aqueous solubility values range from -6.062 to -4.094 which directly indicate all the compounds possess sufficient soluble capabilities in water and escape from blood plasma binding protein and penetrate the biological membrane and produce their effects in therapeutic target site, the MDCK predicted values range from 262 to 1556, human oral absorption percentage ranges from 93 to 100. All the pharmacokinetics parameters are fit well with the acceptable range demarcated for use of human. The results of ADME properties were reported in Table 2.

**Table 2:** Assessment of drug-like properties of the four molecules as verified by QikProp (Schrodinger 10.2).

Compound ID	MW	HBD	HBA	QLogPo/w	Caco-2	QLogHERG	QLogB/B	MDCK	Logs aq	RB	ksha	% Oral absorption
62052	384.46	2	8.5	2.898	529	-5.838	-1.323	323	-4.094	10	-0.092	93
353906	318.37	2	3.5	3.629	1469	-5.013	-0.379	749	-5.123	2	0.551	100
87845	300.36	1	4	3.676	556	-6.534	-1.059	262	-6.062	5	0.442	100
76746	244.29	1	1.5	3.926	2888	-5.752	-0.058	1556	-4.346	2	0.487	100

Molecular weight (<500 Da); Hydrogen bond donors (<5); Hydrogen bond acceptors (<10); Predicted octanol/water partition co-efficient log p (acceptable range: 22.0 to 6.5); Predicted aqueous solubility; S in mol/L (acceptable range: 26.5 to 0.5); Predicted IC50 value for blockage of HERG K<sup>+</sup> channels (acceptable range: below 25.0); Predicted Caco-2 cell permeability in nm/s (acceptable range: 25 is poor and .500 is great); Prediction of binding to human serum albumin (acceptable range: 21.5 to 1.5); QP log BB for brain/blood (-3.0 to 1.2); Predicted percentage of human oral absorption (25 % is poor).

## Molecular dynamics simulation analysis

### Compound 62052

The dynamic behavior of the interaction between hit compound 62052 and JAK2 was investigated by the molecular dynamic simulation package Desmond at different timescales under the physiological state. The protein backbone and ligand RMSD of hit compound 62052 were depicted in Figure 7a. The RMSD of protein backbone exhibited a large deviation in the 16.40 ns and the RMSD value was 2.19 Å, moreover the protein backbone was more stable when the RMSD was reached 1.98 Å in 99.80 ns. The RMSD of both protein backbone and ligand were more stable after 80 ns. Root Mean Square Fluctuations (RMSF) displayed the fluctuations of each protein amino acid residue over the simulation time (Figure 7b). The most fluctuating was found in the following amino acid residue, SER 839, GLY 921, and GLY 1071, and RMSF values were 4.29 Å, 2.91 Å, and 2.76 Å, respectively. Similarly, the backbone more fluctuated in residues SER 839 and GLN 1070, and RMSF values were 4.17 and 2.63 respectively. Besides, the most fluctuated amino acid on the side chain of the protein were ARG 922, GLN 1070, and GLN 1072, and the RMSF values were 4.23 Å, 4.11 Å, and 4.01 Å, respectively. The bar diagram (Figure 7c) of the compound 62052 displayed the main hydrogen bonding, hydrophobic interactions, and water bridge interactions. The hydrogen bond, hydrophobic interactions were observed with LEU 855, LEU 932, and SER 936. Among them, LEU 855 and SER 936 displayed hydrogen bond interactions with a maximum occupancy of 75.1% and 99.1%, respectively, and the hydrophobic interaction was observed with SER 936 with a maximum occupancy of 72.6%. In addition, various intermolecular interactions such as hydrogen bonding, hydrophobic interaction as well as water bridges were formed between compound 62052 with JAK2 kinase domain. Figure 7d shows the hydrogen bonding, hydrophobic interactions that was mainly responsible for the enhancement of the stability of the 62052-JKA2 complex. We identified that the LEU 932, SER 936, and LEU 855 were crucially involved in the formation of hydrogen bonding (99%, 47%, and 71%, respectively) with the active site regions of JAK2 during the simulation period. Moreover, the residues PRO 933 and TYR 931 were predominantly involved in the formation of the water bridge interactions with compound 62052. Interestingly a few more residues such as ALA 880, LEU 855, LUE 983, LEU 932, PRO 933, TYR 931, and VAL 863 were predominantly involved in hydrophobic interactions with compounds 62052 that elevated the binding stability of the protein-ligand complex during the simulation time.

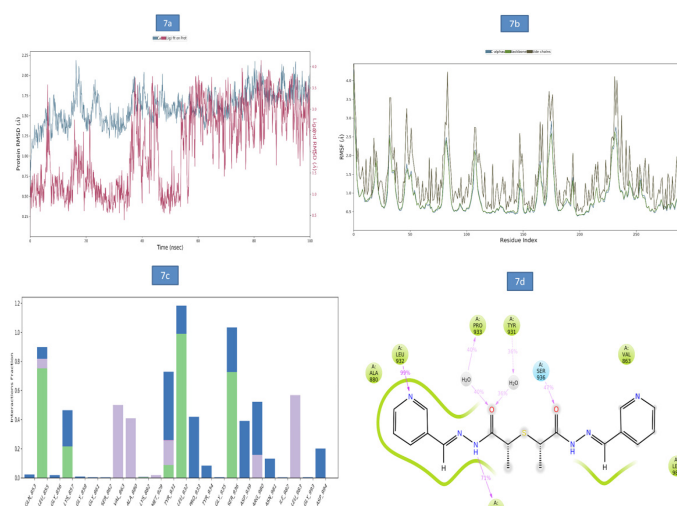


**Figure 7:** (a) The RMSD plot of JAK2-62052 complex during 100ns simulations. (b) The RMSF plot of JAK2-62052 during the 100ns simulations. (c) The bar diagrams of JAK2-62052 contacts during 100ns simulations. (d) The 2d diagram of JAK2-62052 complex at end of the 100ns simulations.

### Compound 353906

The dynamic behavior of the interactions between 353906 and the JAK2 was investigated using the familiar simulation package Desmond at different timescale under physiological state. Figure 8a shows RMSD of the protein and ligand after MD simulation. The RMSD of protein backbone exhibited a large deviation at the 13.30 ns and the RMSD value was 2.44 Å, moreover the protein backbone was more stable when the RMSD were reached 1.82 Å in 99.90 ns. The RMSD of both the protein backbone and the ligand were more stable at end of the simulation in 99 ns when the RMSD reached 1.82 Å. RMSF displayed the fluctuations of each protein amino acid residue over the simulation time period (Figure 8b). The most fluctuating amino acid residue was found to be ARG 922 with a RMSF value of 4.11 Å. The fluctuations also represent the interaction between the protein and the ligand. Similarly, the backbone was more fluctuation in residue ARG 922 and ASN 859, with RMSF values of 3.87 Å and 3.30 Å, respectively. Besides, the most fluctuating amino acid residue on the side chain of the protein was found to be GLN 1070 with a RMSF value of 4.60 Å. The bar diagram (Figure 8c) of compound 353906 displayed mainly hydrogen bonding interactions. The hydrogen bond interactions were observed with GLU 930, LEU 932. Among them, GLU 930 displayed hydrogen bond interaction with a maximum occupancy of 96.2%. In addition, various inter-molecular interactions such as hydrogen bonding, hydrophobic interaction as well as water bridges were formed between the compound 353906 with JAK2

kinase domain. Figure 8d shows the hydrogen bonding, hydrophobic that were significantly responsible for the enhancement the stability of the 353906-JAK2 complex. We identified the negative charged residue GLU 930 and LEU 932 was crucially involved in the formation of hydrogen bonding (96% and 92%, respectively) with active site regions of JAK2 during the simulation period. Moreover, the residue TYR 931 was predominantly involved in the formation of the water bridge interaction with compound 363906. Interestingly a few more residues such as ALA 880, LUE 983, LEU 932, and TYR 931 were predominantly involved in hydrophobic interactions with compound 363902 that elevated the binding stability of the protein-ligand complex during the simulation time.

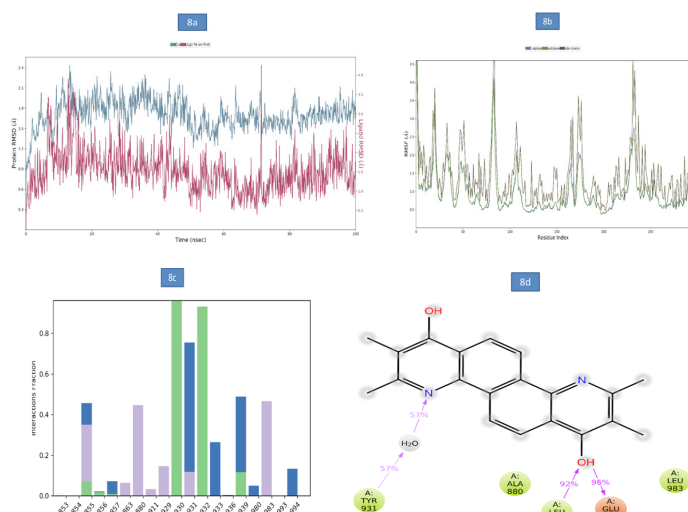


**Figure 8:** (a) The RMSD plot of JAK2-353906 complex during 100ns simulations. (b) The RMSF plot of JAK2-353906 during the 100ns simulations. (c) The bar diagrams of JAK2-353906 contacts during 100ns simulations. (d) The 2d diagram of JAK2-353906 complex at end of the 100ns simulations.

### Compound 87845

The dynamic behavior of the interaction between compound 87845 and the JAK2 was investigated by the familiar simulation package Desmond at different timescale under the physiological state. Figure 9a shows RMSD of the protein and ligand. The RMSD of protein backbone exhibited a slight deviation in 62.70 ns and the RMSD values were 2.68 Å, moreover the protein backbone was more stable when the RMSD was reached 2.24 Å. The deviation in ligand RMSD between the 0.20 to 19 ns was found in the ranges of 1.15 Å to 2.42 Å, but the ligand most stable unless the ligand RMSD finally reached 2.54 Å. The RMSF displayed the fluctuations of each protein amino acid residue over the simulation time period (Figure 9b). The fluctuation also represents the interaction between the protein and the ligand. Initially a slight fluctuation was observed in backbone of the protein residue THR 842 and ASN 852, and the RMSF values were 3.3 Å and 2.87 Å respectively. Large fluctuations were observed in the side chain of protein residue THR 842 and the RMSF value was 4.45 Å. The bar diagram (Figure 9c) of the compound 87845 displayed the main hydrogen bonding, hydrophobic interactions, and water bridge interactions. The hydrophobic and hydrogen bond interaction were observed with GLU 930, LEU 932 with a maximum occupancy of 1.898% and 57.3%, respectively. In addition, various intermolecular interactions such as hydrogen bonding and water bridges were formed between compound 87845 with JAK2 kinase domain. Figure 9d shows the hydrogen bonding plays a crucial role in the enhancement of the stability of the 87845-JAK2 complex. The LEU 932 was

involved in the formation of hydrogen bonding (95%) with the active site region of JAK2 during the simulation period. Moreover, the negative charged residue GLU 930 was predominantly involved in the formation of the water bridge interaction with compound 87845. Furthermore, only LEU 932 was involved in hydrophobic interactions with compound 87845 to enhance the binding stability of the protein-ligand complex during the simulation time.

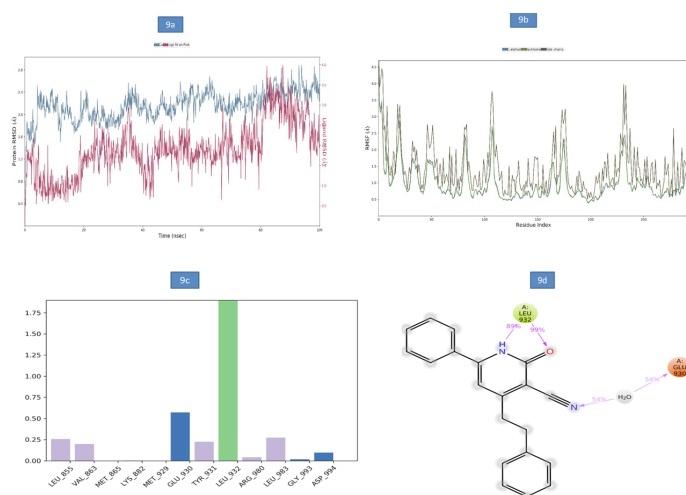


**Figure 9:** (a) The RMSD plot of JAK2-87845 complex during 100ns simulations. (b) The RMSF plot of JAK2-87845 during the 100ns simulations. (c) The bar diagrams of JAK2-87845 contacts during 100ns simulations. (d) The 2d diagram of JAK2-87845 complex at end of the 100ns simulations.

### Compound 76746

We investigated the binding stability of the JAK2 with compound 76746. Fig. 10a shows RMSD of the protein and the ligand. The RMSD of protein backbone exhibited a slight deviation between 45.30 ns and 77.30 ns and the RMSD values were from 2.38 Å to 2.54 Å. Slight changes in the ligand RMSD was observed from 1ns to 95ns, and larger deviation in ligand RMSD was observed at 95 ns and the ligand RMSD was reached 3.44 Å. RMSF displayed the fluctuations of each protein amino acid residue over the simulation time period (Fig. 10b). The most fluctuating amino acid residue was found to be ASN 859, GLU 1012, GLU 1015 and RMSF values were 3.44 Å, 4.19 Å, and 4.23 Å, respectively. The backbone more fluctuated in residue ASN 859, and RMSF value was 3.49 Å. Besides, the most fluctuated amino acids on the side chain of the protein were GLU 1012 and GLU 1015 and the RMSF values were 4.19 Å and 4.23 Å, respectively. The bar diagram (Figure 10c) of the compound 76746 displayed the main hydrogen bonding and water bridge interactions. The hydrogen bond, water bridge interactions were observed with LEU 932 and ALA 880. The LEU 932 displayed hydrogen bond interaction with a maximum occupancy of 95.3% and the water bridge interaction was observed with ALA 880 with a maximum occupancy of 60.0%. In this complex only one hydrogen bonding and one hydrophobic interaction were formed between compound 76746 and the JAK2 kinase domain. Figure 5d shows the hydrogen bonding, hydrophobic interactions that were mainly responsible for enhancing the binding stability of 76746-JKA2 complex. We identified that the LEU 932 were crucially involved in the formation of hydrogen bonding (95%) with the active site region of JAK2 during the simulation period. A few more residues such as ALA 880, LEU 855, LUE 983, LEU 932 and TYR 931 were predominantly involved in hydrophobic interactions with

compounds 76746 that elevated the binding stability of the protein-ligand complex during the simulation time.

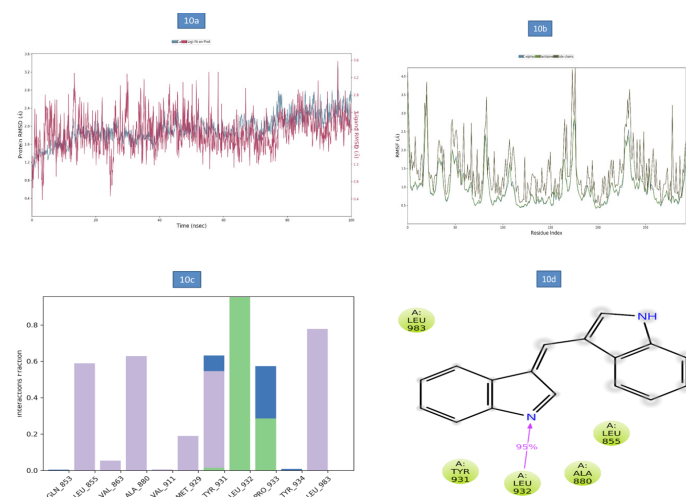


**Figure 10:** (a) The RMSD plot of JAK2-76746 complex during 100ns simulations. (b) The RMSF plot of JAK2-76746 during the 100ns simulations. (c) The bar diagrams of JAK2-76746 contacts during 100ns simulations. (d) The 2d diagram of JAK2-76746 complex at end of the 100ns simulations.

## Conclusion

Rheumatoid arthritis is a chronic autoimmune disease primarily affecting in elder women. Janus kinase 2, of the Janus kinase family, is a non-receptor tyrosine kinase predominantly implicated in the activation of the crucial JAK/STAT signaling pathway. Aberrant activity of the JAK/STAT signaling pathway can lead to RA. Here, we endeavored to find effective inhibitors against JAK2 to offer better therapeutic options for RA. We employed structure-based virtual screening of the NCI database against JAK2. We began with docking 250,000 molecules from the database with JAK2 using Schrödinger Glide HTVS mode, 50,000 molecules were then filtered from the HTVS results and subjected to SP mode for further ligand scrutinization, the top scoring 5,000 compounds were then funneled from SP mode and docked using XP mode resulting in 50 potential molecules that surpassed the glide XP score of the natural JAK2 ligand. The 50 molecules were then evaluated for drug likeness properties. Finally, we found four compounds having adequate predicted ADME properties. Furthermore, to investigate binding conformational stability of the four-potential drug-like molecules we studied the molecular dynamics using Desmond. The molecular dynamics simulation investigation reveals that all four hit molecules are more stable inside the binding pocket of the JAK2 kinase domain at the end of the simulation and inhibits the over expression of the kinase activity of JAK2. Based on this *in silico* study, the four molecules showed great potential for further lead optimization and are suggested to undergo further pre-clinical and clinical investigations.

## Declaration

**Acknowledgement:** I would like to thank to Department of Biotechnology, Selvam Arts and Science College (Autonomous), Namakkal for providing lab facilities as well as encouragement for this study.

**Author contributions:** Conceived and designed the experiments: AM, WJ, AJ. Performed the experiments: AM. Analyzed the data: AM, WJ. Contributed software facility: AM. Wrote the paper: AM, H.-F.J., WJ. Assisted in writing the paper and refer-

encing: H.-F. J, WJ.

**Conflict of interest:** The authors declare that they have no competing interests.

**Compliance with ethical standards:** Not applicable. The ethical standards have been met.

**Funding:** This compilation is a research article written by its author and required no substantial funding to be stated.

**Data availability:** From corresponding authors upon request.

## References

- Jacqueline Bullock, Syed AA Rizvi, Ayman M Saleh, Sultan S Ahmed, Duc P Do, et al. Rheumatoid Arthritis: A Brief Overview of the Treatment. *Med Princ Pract.* 2018; 27: 501-507.
- Xinqiang Song, Qingsong Lin. Genomics, transcriptomics and proteomics to elucidate the pathogenesis of rheumatoid arthritis. *Rheumatol Int.* 2017; 37: 1257-1265.
- Sana Iqbal, Mohammad A Rattu. Neal Shah Review of Rheumatoid Arthritis. *US Pharm (Specialty&Oncologysuppl).* 2019; 44: 8-11.
- Min Hu, Chengbo Xu, Chao Yang, Hongli Zuo, Chengjuan Chen, et al. Discovery and evaluation of ZT55, a novel highly-selective tyrosine kinase inhibitor of JAK2V617F against myeloproliferative neoplasms. *J Exp Clin Cancer Res.* 2019; 38: 49.
- Paolo Catarsi, Vittorio Rosti, Giacomo Morreale, Valentina Pioletto, Laura Villani, et al. JAK2 Exon 14 Skipping in Patients with Primary Myelofibrosis: A Minor Splice Variant Modulated by the JAK2-V617F Allele Burden. *PLoS One.* 2015; 10: e0116636.
- Olli Silvennoinen, Daniela Ungureanu, Yashavanthi Niranjan, Henrik Hammaren, Rajintha Bandaranayake, et al. New insights into the structure and function of the pseudokinase domain in JAK2. *Biochem Soc Trans.* 2013; 41: 1002-1007.
- Kavitha Gnanasambandan and Peter P Sayeski. A Structure-Function Perspective of Jak2 Mutations and Implications for Alternate Drug Design Strategies: The Road not Taken. *Curr Med Chem.* 2011; 18: 4659-4673.
- Wanqi Wang, Yanyan Diao, Wenjie Li, Yating Luo, Tingyuan Yang, et al. Design, synthesis and structure-activity relationship study of aminopyridine derivatives as novel inhibitors of Janus kinase 2. *Bioorg Med Chem Lett.* 2019; 29: 1507-1513.
- Annina T Virtanen, Teemu Haikarainen, Juuli Raivola, Olli Silvennoinen. Selective JAKinibs: Prospects in Inflammatory and Autoimmune Diseases. *BioDrugs.* 2019; 33: 15-32.
- Fabienne Baffert, Catherine H Régnier, Alain De Pover, Carole Pissot-Soldermann, Gisele A Tavares, et al. Potent and selective inhibition of polycythemia by the quinoxaline JAK2 inhibitor NVP-BSK805. *Mol Cancer Ther.* 2010; 9: 1945-1955.
- G Madhavi Sastry, Matvey Adzhigirey, Tyler Day, Ramakrishna Annabhimoju et al. Protein and ligand preparation: parameters, protocols, and influence on virtual screening enrichments. *Journal of Computer-Aided Molecular Design.* 2013; 2: 221-234.
- Evanthia Lionta, George Spyrou, Demetrios K Vassilatis and Zoe Cournia. Structure-Based Virtual Screening for Drug Discovery: Principles, Applications and Recent Advances. *Curr Top Med Chem.* 2014; 14: 1923-1938.
- Reham Adnan Al-Ansari, Rita S Elias and Shaker AN Aljadaan. Synthesis, Ant Proliferative Activity and Docking Study of New Quercetin Derivatives against MDA-MB231 Breast Cancer Cell Lines. *American Journal of Applied Sciences.* 2019; 16: 143-161.

14. Tony Eight Lin, Wei-Chun Huang Fu, Min-Wu Chao, Tzu-Ying Sung, Chao-Di Chang, et al. A Novel Selective JAK2 Inhibitor Identified Using Pharmacological Interactions. *Front Pharmacol*. 2018; 9: 1379.
15. Dik-Lung Ma, Daniel Shiu-Hin Chan, Guo Wei, Hai-Jing Zhong, Hui Yang, et al. Virtual screening and optimization of Type II inhibitors of JAK2 from a natural product library. *Chem Commun (Camb)*. 2014 50: 13885-13888.
16. Kh Dhanachandra Singh, Muthusamy Karthikeyan, Palani Kirubakaran, Selvaraman Nagamani. Pharmacophore filtering and 3D-QSAR in the discovery of new JAK2 inhibitors *J Mol Graph Model*. 2011; 30: 186-197.
17. Downloadable Structure Files of NCI Open Database Compounds. 2020.
18. Swaysiddha Tripathy, Mohammed Afzal Azam, Srikanth Jupudi, Susanta Kumar Sahu. Pharmacophore generation, atom-based 3D-QSAR, molecular docking and molecular dynamics simulation studies on benzamide analogues as FtsZ inhibitors. *J Biomol Struct Dyn*. 2018; 36: 3218-3230.
19. Mohan Anbuselvam, Muruges Easwaran, Arun Meyyazhagan, Jeeva Anbuselvam, Haripriya Kuchi Bhotla, et al. Structure-based virtual screening, pharmacokinetic prediction, molecular dynamics studies for the identification of novel EGFR inhibitors in breast cancer. *J Biomol Struct Dyn*. 2020; 22; 1-10.
20. Neeraj Kumar, Shashank Shekhar Mishra, Chandra Shekhar Sharma, Hamendra Pratap Singh, Sourav Kalra. In silico binding mechanism prediction of benzimidazole based corticotropin releasing factor-1 receptor antagonists by quantitative structure activity relationship, molecular docking and pharmacokinetic parameters calculation. *J Biomol Struct Dyn*. 2018; 36: 1691-1712.
21. Rohitash Yadav, Mohammed Imran, Puneet Dhamija, Dheeraj Kumar Chaurasia, and Shailendra Handu Virtual screening, ADMET prediction and dynamics simulation of potential compounds targeting the main protease of SARS-CoV-2. *J Biomol Struct Dyn*. 2020: 1-16.
22. David S Wishart. Improving early drug discovery through ADME modelling: an overview. *Drugs RD*. 2007; 8: 349-362.
23. Joseph A DiMasi, Henry G Grabowski, Ronald W Hansen. Innovation in the pharmaceutical industry: New estimates of R&D costs. *J Health Econ*. 2016; 47: 20-33.
24. Jie Dong, Ning-Ning Wang, Zhi-Jiang Yao, Lin Zhang, Yan Cheng, et al. ADMETlab: a platform for systematic ADMET evaluation based on a comprehensively collected ADMET database. *J Cheminform*. 2018; 10: 29.
25. FideleNtie-Kang. Aninsilico evaluation of the ADMET profile of the StreptomeDB database. *Springerplus*. 2013; 2: 353.
26. Banoth Karan Kumar, Faheem, Kondapalli Venkata Gowri Chandra Sekhar, Rupal Ojha, Vijay Kumar Prajapati, Aravinda Pai, et al. Pharmacophore based virtual screening, molecular docking, molecular dynamics and MM-GBSA approach for identification of prospective SARS-CoV-2 inhibitor from natural product databases. *J Biomol Struct Dyn*. 2020; 1-24.
27. Schrödinger Release 2020-2021. Desmond Molecular Dynamics System, D. E. Shaw Research, New York, NY, 2020. Maestro-Desmond Interoperability Tools, Schrödinger, New York, NY, 2020.
28. Ramin Ekhteiari Salmas, Ayhan Unlu, Muhammet Bektaş, Mine Yurtsever, Mert Mestanoglu et al. Virtual Screening of Small Molecules Databases for Discovery of Novel PARP-1 Inhibitors: Combination of in silico and in vitro Studies. *J Biomol Struct Dyn*. 2017; 35: 1899-1915.
29. Ganesh Kumar Veeramachaneni, K Kranthi Raj, Leela Madhuri Chalasani, Jayakumar Singh Bondili, Venkateswara Rao Talluri. High-throughput virtual screening with e-pharmacophore and molecular simulations study in the designing of pancreatic lipase inhibitors. *Drug Des Devel Ther*. 2015; 9: 4397-4412.